AD

TECHNICAL REPORT ARCCB-TR-96024

STRESS CONCENTRATION, STRESS INTENSITY, AND FATIGUE LIFETIME CALCULATIONS FOR SHRINK-FIT COMPOUND TUBES CONTAINING AXIAL PERFORATIONS WITHIN THE WALL

STEPHEN N. ENDERSBY
ANTHONY P. PARKER
TIMOTHY J. BOND
JOHN H. UNDERWOOD

AUGUST 1996

US ARMY ARMAMENT RESEARCH,
DEVELOPMENT AND ENGINEERING CENTER
CLOSE COMBAT ARMAMENTS CENTER
BENÉT LABORATORIES
WATERVLIET, N.Y. 12189-4050

DISCLAIMER NOTICE

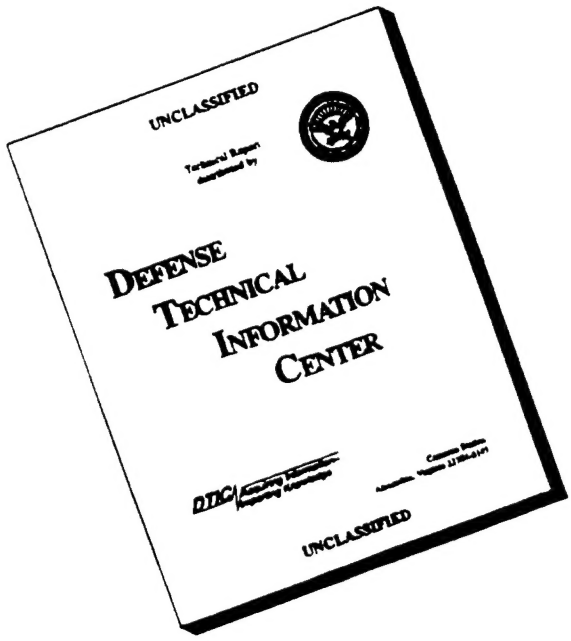

THIS DOCUMENT IS BEST QUALITY AVAILABLE. THE COPY FURNISHED TO DTIC CONTAINED A SIGNIFICANT NUMBER OF PAGES WHICH DO NOT REPRODUCE LEGIBLY.

DISCLAIMER

The findings in this report are not to be construed as an official Department of the Army position unless so designated by other authorized documents.

The use of trade name(s) and/or manufacturer(s) does not constitute an official indorsement or approval.

DESTRUCTION NOTICE

For classified documents, follow the procedures in DoD 5200.22-M, Industrial Security Manual, Section II-19 or DoD 5200.1-R, Information Security Program Regulation, Chapter IX.

For unclassified, limited documents, destroy by any method that will prevent disclosure of contents or reconstruction of the document.

For unclassified, unlimited documents, destroy when the report is no longer needed. Do not return it to the originator.

REPORT DOCUMENTATION PAGE

Form Approved
OMB No. 0704-0188

1. AGENCY USE ONLY (Leave blank)	2. REPORT DATE	3. REPORT TYPE AND DATES COVERED
	August 1996	Final

4. TITLE AND SUBTITLE
STRESS CONCENTRATION, STRESS INTENSITY, AND FATIGUE LIFETIME CALCULATIONS FOR SHRINK-FIT COMPOUND TUBES CONTAINING AXIAL PERFORATIONS WITHIN THE WALL

5. FUNDING NUMBERS
AMCMS No. 6111.02.H611.1

6. AUTHOR(S)
Stephen N. Endersby (Univ. of Northumbria, UK), Anthony P. Parker (Royal Military College of Science, Cranfield Univ., UK), Timothy J. Bond (Univ. of Northumbria, UK), and John H. Underwood

7. PERFORMING ORGANIZATION NAME(S) AND ADDRESS(ES)
U.S. Army ARDEC
Benet Laboratories, AMSTA-AR-CCB-O
Watervliet, NY 12189-4050

8. PERFORMING ORGANIZATION REPORT NUMBER
ARCCB-TR-96024

9. SPONSORING / MONITORING AGENCY NAME(S) AND ADDRESS(ES)
U.S. Army ARDEC
Close Combat Armaments Center
Picatinny Arsenal, NJ 07806-5000

10. SPONSORING / MONITORING AGENCY REPORT NUMBER

11. SUPPLEMENTARY NOTES
Presented at the 28th National Symposium on Fatigue and Fracture, Saratoga, NY, 25-27 June 1996.
Published in proceedings of the symposium.

12a. DISTRIBUTION / AVAILABILITY STATEMENT
Approved for public release; distribution unlimited.

12b. DISTRIBUTION CODE

13. ABSTRACT *(Maximum 200 words)*

Elastic-plastic numerical stress analyses and fatigue lifetime predictions are presented for shrink-fit compound tubes containing multiple, axial holes at the interface between inner and outer tube. The holes, which are semi-circular, are introduced initially as periodic notches on the outer surface of the inner tube and an outer plain tube is heated, slid over the inner tube, and allowed to cool to achieve the shrink-fit. Residual stresses resulting from interference and operational stress ranges arising from cyclic bore pressurization are calculated and fatigue lifetimes are predicted. Two potentially critical locations for fatigue failure are identified as the bore and the notch root. The predicted lifetimes are compared with earlier work on a similar overall geometry subjected to autofrettage. The critical location is shown to be at the bore and a clear improvement in overall fatigue lifetime is demonstrated for the shrink-fit tube compared with the autofrettaged tube. As the interface radius is reduced, there is a general reduction in the ratio of fatigue stress range at the bore to that at the hole and the possibility of the critical location moving to the notch root. A normalized presentation for design purposes is proposed.

14. SUBJECT TERMS
Crack Growth, Fatigue Cracks, Fatigue Lifetimes, Axial Holes, Channels, Compound Tubes, Cylinders, Compound Cylinders, Fracture (Materials), Fracture Mechanics, Residual Stress, Shrink-Fit, Stress Concentration Factor, Stress Intensity Factor

15. NUMBER OF PAGES
12

16. PRICE CODE

17. SECURITY CLASSIFICATION OF REPORT	18. SECURITY CLASSIFICATION OF THIS PAGE	19. SECURITY CLASSIFICATION OF ABSTRACT	20. LIMITATION OF ABSTRACT
UNCLASSIFIED	UNCLASSIFIED	UNCLASSIFIED	UL

TABLE OF CONTENTS

TABLES

LIST OF ILLUSTRATIONS

INTRODUCTION

The use of autofrettage to enhance fatigue lifetimes of thick cylinders subjected to internal cyclic pressurization is well known and relatively well understood. Recent work has addressed the problems associated with geometrical changes which remove the initial axi-symmetric nature of geometry and stressing of these tubes, namely:

a. Axial erosion grooves, *which arise after autofrettage,*along the bore of the tube, Ref [1].
b. Cross-bore holes normal to the tube axis [2] and inclined at an angle to the axis [3]. These holes likewise are *introduced after autofrettage.*
c. Periodic axial holes within the bore which are *introduced prior to autofrettage* of the tube [4].

The purpose of the work presented herein is to predict, using elastic and elastic/plastic stress analysis methods, the fatigue behavior of compound cylinders which contain a series of equally-spaced holes oriented parallel to the tube axis, the holes being created by the thermal shrink-fitting of an external (plain) tube onto an externally-notched inner tube, Fig. 1. Experience indicates that two potentially critical failure locations are on a radial line at the point on the hole closest to the bore and on the bore itself.

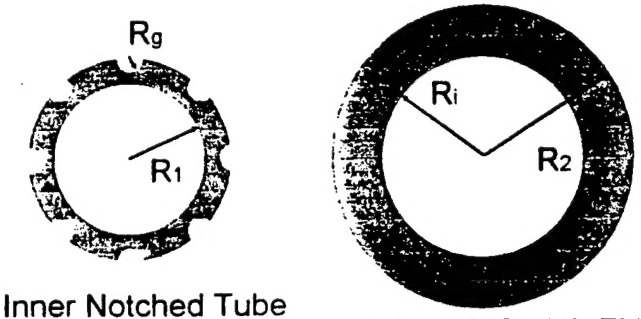

Fig. 1 : Hole Geometries Analyzed Using Finite Element Method

ELASTIC FINITE ELEMENT ANALYSIS

Several possible designs were analyzed using the NISA Finite Element program. In all cases they consist of a cyclic array of 24 equally-spaced holes. The material had an Elastic Modulus, E, of 200GPa and a coefficient of thermal expansion, α, of 12×10^{-6}/degC; in cases of autofrettage used for comparison purposes a yield strength of 1200MPa was employed.

Throughout the investigation the inner and outer radii (R_1 and R_2) were 84.5mm and 152.5mm respectively. The groove radius (R_g) was 6.35mm. Interface radii (R_i) for the cases considered are given in Table 1 below:

Table 1 : Interface Radii Examined

Case 1: Interface radius (R) 122.00mm
Case 2: Interface radius (R) 114.00mm
Case 3: Interface radius (R) 106.75mm
Case 4: Interface radius (R) 100.65mm

In order to construct an FE mesh for these configurations taking full advantage of symmetries it was only necessary to model some 360/(24x2) or 7.5 degrees of the tube. Essential symmetry conditions were ensured by imposing zero shear stress and zero tangential displacement on all radii of symmetry. The interference was simulated in the FE analysis by maintaining a constant temperature difference between material in each of the inner and outer tubes.

One particular objective of this work was to compare the shrink fit method with the alternative of autofrettage examined in Ref [4]. Three different amounts of shrink fit were investigated for each of the four interface radii. The shrink fits were designed to give a hoop stress at the bore of two shrink-fit plain cylinders equivalent to 40%, 50% and 60% autofrettage (overstrain) of a solid tube respectively.These temperature differentials were selected to give an appropriate spread of results for comparison purposes, whilst avoiding significant amounts of plasticity at the hole boundary. The relationships between equivalent autofrettage, interference and temperature differential are shown in Table 2.

Table 2 : Relationship Between Equivalent Autofrettage, Interference and Temperature Differential for Tubes Examined

	Equiv. Autofrettage	Interference	Temp diff
Case 1	40%	0.6627mm	452.65deg C
	50%	0.7828mm	534.72deg C
	60%	0.8508mm	581.15deg C
Case 2	40%	0.5004mm	365.8deg C
	50%	0.5911mm	432.1deg C
	60%	0.6424mm	469.6deg C
Case 3	40%	0.4008mm	312.9deg C
	50%	0.4735mm	369.6deg C
	60%	0.5146mm	401.7deg C
Case 4	40%	0.3512mm	290.8deg C
	50%	0.4150mm	343.6deg C
	60%	0.4510mm	373.4deg C

To simulate cyclic pressurization a pressure of 434.4 MPa was applied to the bore.

ELASTIC HOOP STRESSES DUE TO BORE PRESSURIZATION AND SHRINK FIT

Fig. 2 shows(upper curve) the elastic variation of hoop stress with radius from the bore to the notch root for an internal pressure of 434.4MPa. For comparison the standard (Lamé) solution for a pressurized, plain thick cylinder is also shown. This indicates the expected stress concentration effect of the notch and a slight variation at the bore resulting from the presence of the holes, see [4] for a discussion of this point.

Fig. 2 also illustrates (lower three curves) the compressive hoop stresses resulting from the shrink fitting process. These results were obtained from an elastic analysis using NISA, and it is clear that no compressive yielding is likely for Cases 1 and 2 since maximum hoop stress magnitude does not exceed yield strength (1200 MPa). Elastic/plastic analyses were also conducted for those cases of shrink-fitting in which yielding might occur; these results are referred to later in this paper. For comparison the more complex residual stress'profiles resulting from an elastic/plastic FE analysis of autofrettage of the same geometry [4] are also presented in Figure 2 as the middle three curves; note that these results relate to equivalent overstrains of 40%, 60% and 80%.

HOOP STRESS RANGE AND FATIGUE LIFETIME

Superposition of the combinations of elastic stresses due to internal pressure and residual stresses arising from shrink-fitting provides an indication of the positive stress range during cyclic pressurization, Fig. 3.

There are two potential fatigue failure locations on a single radial line at the point on the hole closest to the bore and at the bore itself. The fatigue lifetime formulae, based upon Paris' law and governing lifetime for failure from different initial defect sizes with different stress ranges are developed in [5] . In summary the fatigue lifetime at a particular location depends principally upon initial defect size (a_i) and stress range ($\Delta\sigma$), the latter taking account of both residual stresses and any pressure acting upon the crack surfaces as a result of infiltration from the bore. The expression for lifetime, N, is:

$$N = \frac{a_i^{(1-m/2)}}{C\pi^{m/2}(m/2-1)(\Delta\sigma)^m} \qquad (1)$$

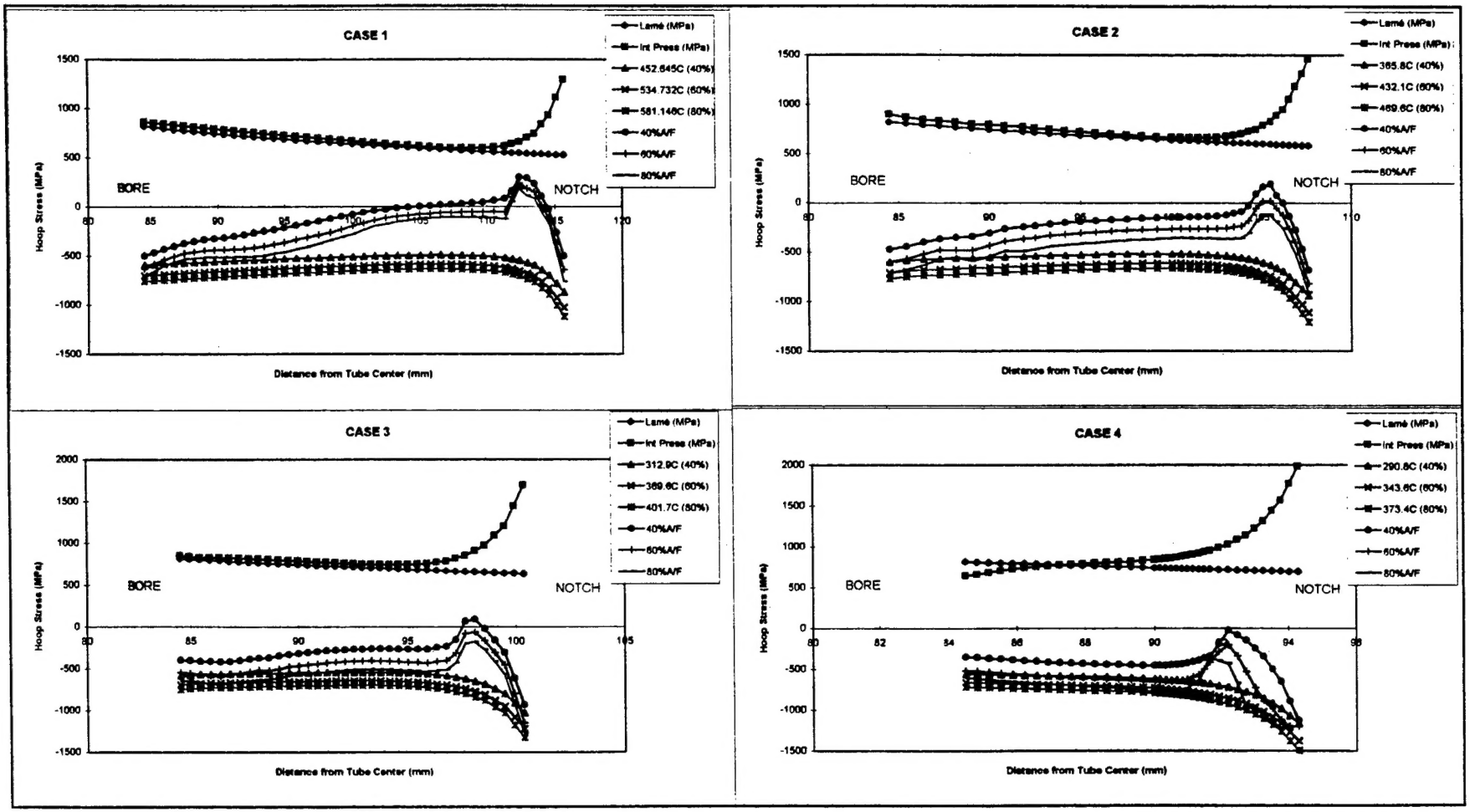

Figure 2: Elastic Variation of Hoop Stress from Bore to Hole due to Internal Pressure (upper two curves for each case); Residual Hoop Stresses Arising from Shrink Fitting (lower three curves); and from Autofrettage (middle three curves).

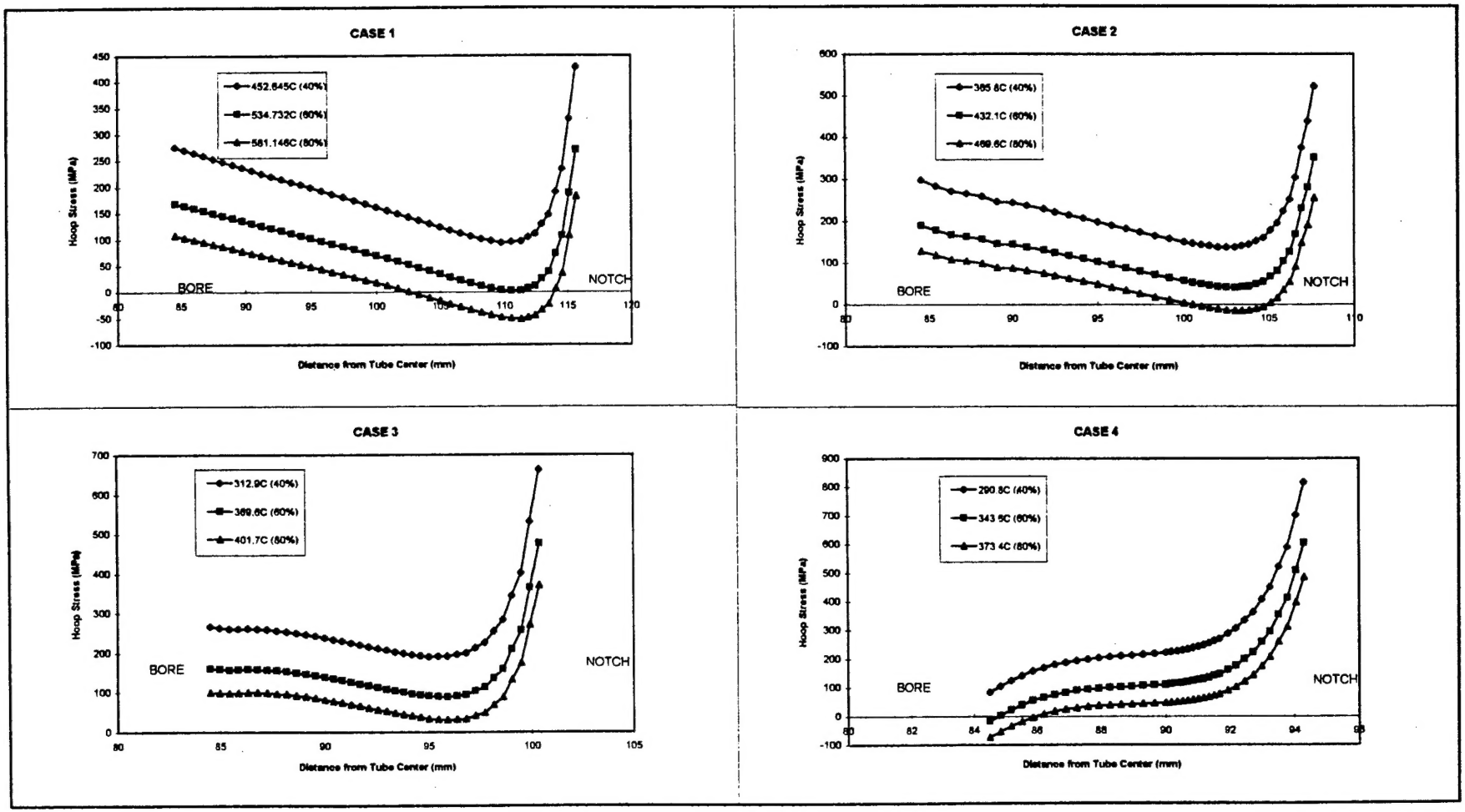

Figure 3: Positive Cyclic Stress Range of Shrink-Fit Arrangement Resulting from Pressurization of Bore

where C and m are Paris' Law coefficient and exponent respectively.

For design purposes, where there are two potential failure locations, it may be more useful to plot lifetime ratios. If we calculate the ratio of lifetimes with two different initial crack lengths and associated stress ranges, a_1 and $\Delta\sigma_1$, a_2 and $\Delta\sigma_2$, these combinations will, in general, yield two different lifetimes, N_1 and N_2. From Equation (1) the ratio of these lifetimes is:

$$\frac{N_2}{N_1} = \left[\frac{a_2}{a_1}\right]^{(1-m/2)} \left[\frac{\Delta\sigma_1}{\Delta\sigma_2}\right]^{m} \qquad (2)$$

The effective stress range at the hole is given in Fig. 3 by the values at the far right of each plot, whilst the effective stress range at the bore is that given in Figure 3 at the left *plus the contribution from the bore pressure which infiltrates the fatigue crack*. Assuming at this stage equal length initial defects at the two locations, the more critical will be that with the higher effective stress range. Table 3 gives ratios, for all geometries analyzed, of effective stress range at bore/effective stress range at hole, designated Fatigue Stress Range Ratio, R_σ where:

$$R_\sigma = \frac{\textit{(Hoop Stress Range at Bore + Bore Pressure)}}{\textit{Hoop Stress Range at Notch}} \qquad (3)$$

When R_σ is below unity this indicates a potential shift of failure location from bore to hole for the case of equal length initial defects at the two locations. In the general case where $a_B \neq a_H$ Equation (2) indicates that the shift will occur when:

$$R_\sigma = \left[\frac{a_B}{a_H}\right]^{(1/m-1/2)} \qquad (4)$$

where a_B and a_H are the initial crack sizes at the bore and the hole respectively.

Table 3 shows the R_σ ratio for shrink-fitting for all cases considered. For all geometries the result of the elastic analysis is provided. In cases of shrink-fitting in which yielding occurs the value in parentheses refers to the equivalent elastic/plastic FE analysis result. For comparison Table 3 also includes full results of the elastic/plastic autofrettage FE analysis reported in detail in [4]. Furthermore, since there is experimental evidence that, for the autofrettage case, the residual stresses at the hole may be near to zero, a further set of ratios based on this assumption is included.

Table 3 : Fatigue Stress Range Ratios for Shrink Fit Analysis, Autofrettage Analysis and Autofrettage Experiment

	Equivalent Autofrettage	Shrink - Fit	Autofrettage (Analysis)	Autofrettage (zero residual stress)
Case 1	40%	1.62	1	1.21
	50%	2.19	–	–
	60%	2.96	1.02	1.01
	80%	–	1.10	0.89
Case 2	40%	1.40	1.10	0.59
	50%	1.77	–	–
	60%	2.20	1.13	0.50
	80%	–	1.12	0.43
Case 3	40%	1.06	1.17	0.53
	50%	1.25 (1.21)	–	–
	60%	1.44 (1.09)	1.35	0.44
	80%	–	1.53	0.38
Case 4	40%	0.64	0.85	0.37
	50%	0.69 (0.53)	–	–
	60%	0.74 (0.46)	0.72	0.28
	80%	–	0.61	0.24

Note 1: Shrink-fit results are predominantly elastic. Where yielding occurs the equivalent elastic/plastic result is given in parentheses.
Note 2: See Ref [4] for full details of autofrettage analyses

It is important to note that the differences between predicted and measured residual stresses at the hole reported in [4] arise from elastic/plastic assumptions which do not fully represent the actual notch effects. In the case of the shrink-fitting process, which is overwhelmingly elastic in nature and in which reversed yielding does not occur, such problems do not arise.

In fact the assumption of equal initial defect sizes at hole and bore is far from reality, since in the application under consideration (a large caliber gun tube) the initial crack depth at the bore due to heat-checking is likely to be several times larger than that at the hole.

In the case of autofrettage there is some evidence that failure may initiate from the hole in cases of over 60% autofrettage (overstrain) (Ref [4]). In the case of

shrink-fit it appears that the critical location will undoubtedly be the bore; there are two reasons for this assertion:

a. The fatigue stress range is higher at the bore for Cases 1, 2 and 3

b. The initial defect sizes are larger at the bore (at least twenty times greater than at the hole, [4]). Referring to Equation (4) it is noted that with such a ratio of initial defect sizes, failure will occur from the bore down to a fatigue stress ratio of 0.61, assuming a Paris law exponent, m = 3. Clearly such a figure is not achieved in any of the shrink-fit cases under consideration.

This observation leads to a straightforward prediction of fatigue lifetime for the shrink-fit design of Case 2 which has the same value of a_i as the autofrettage design. Since there are laboratory lifetime figures available for failures originating from the bore of heat-checked cannon tubes made of the same material, [4], Equation (2) indicates that, for such equal initial crack sizes, the predicted lifetime is given by:

Lab Lifetime x (Lab Effective Stress range / New Effective Stress range)^m (5)

Some existing data is provided in Table 4, and used to predict lifetimes for Case 2. This is further compared with experimental data relating to failure from the hole in the autofrettaged design; in the latter case a ratio $a_B/a_H = 58.8$ is assumed in accordance with [4].

In the case of the 60% overstrain of a plain tube, the tube was subjected to a cyclic bore pressure of 393 MPa resulting in a positive bore stress range of 717.8 MPa. Prior to cyclic pressurization the tube had been fired sufficiently for initial bore heat-check cracking to be fully established. Thus the initial crack size at the bore may be assumed to be the same in other heat-checked tubes. In the case of shrink-fitting, with failure from the bore, a simple application of Equation (5) provides the predicted lifetimes shown in Table 4.

Turning to the case of autofrettage, with failure from the hole, Ref [4] contains details of the calculation of the ratio a_B/a_H where a_B relates to heat-checking and a_H relates to surface finish. The a_B/a_H ratio calculated in [4] is 58.8. Equation (2) then provides a lifetime prediction of 9,005 cycles with cyclic pressurization of 434 MPa. This lifetime is the same for all percentage overstrains since it is observed experimentally, [4], that residual hoop stress at the hole is near zero.

An additional objective of this work was to determine whether, by adjusting the semi-circular groove shape, effectively making it a semi-ellipse with a reduced radius of curvature at the critical location, there would be any improvement in

lifetime. The conclusion is clear, since the notch is not the primary fatigue failure location, any reduction in the local stresses will have no effect upon an overall lifetime which is governed by failure from a relatively remote location, namely the bore.

Table 4 : Predicted Lifetimes for Proposed Shrink-Fit design (Case 2)

60% overstrain of plain tube - Experimental result; (Ref 4)				
Stress range (MPa) (B)	717.8			
Life (Cycles)	10,873			
Shrink Fitting - Predicted Lifetimes of Perforated Tube;				
Equivalent Autofrettage (%)	40%	50%	60%	–
Stress range (MPa) (B)	732.44	624.02	562.7	–
Life (Cycles) (B)	10,234	16,549	22,570	–
Autofrettage - Predicted Lifetime for All % overstrains of perforated tube (based upon experimental result); Ref 4				
Equivalent Autofrettage (%)	40%	–	60%	80%
Stress Range (MPa) (H)	1511	–	1511	1511
Life (Cycles) (H)	9,005	–	9,005	9,005

Notes:
1. All predicted lifetimes are for Case 2 geometry and loading with cyclic bore pressure of 434 MPa
2. (B) indicates failure originating from bore
3. (H) indicates failure originating from hole
4. a_B/a_H = 58.8 throughout (Ref 4)

A NORMALIZED, PARAMETRIC DESIGN REPRESENTATION

For future design purposes it may be more appropriate to present the results herein in normalized form, since by varying the major parameters (amount of shrink-fit and radius of interface) the crucial fatigue stress range ratio, R_σ, will vary and may cause the critical location to shift from bore to hole. Fig. 4 shows the variation of R_σ with normalized interface radius, R_N, and normalized interface pressure, P_N, where:

$$R_N = (Ri - R1)/(R2 - R1) \qquad \text{and} \qquad P_N = E\alpha T/P$$

where P is pressure acting upon bore and bore crack surfaces. Note that all results presented in normalized form are based upon elastic analyses.

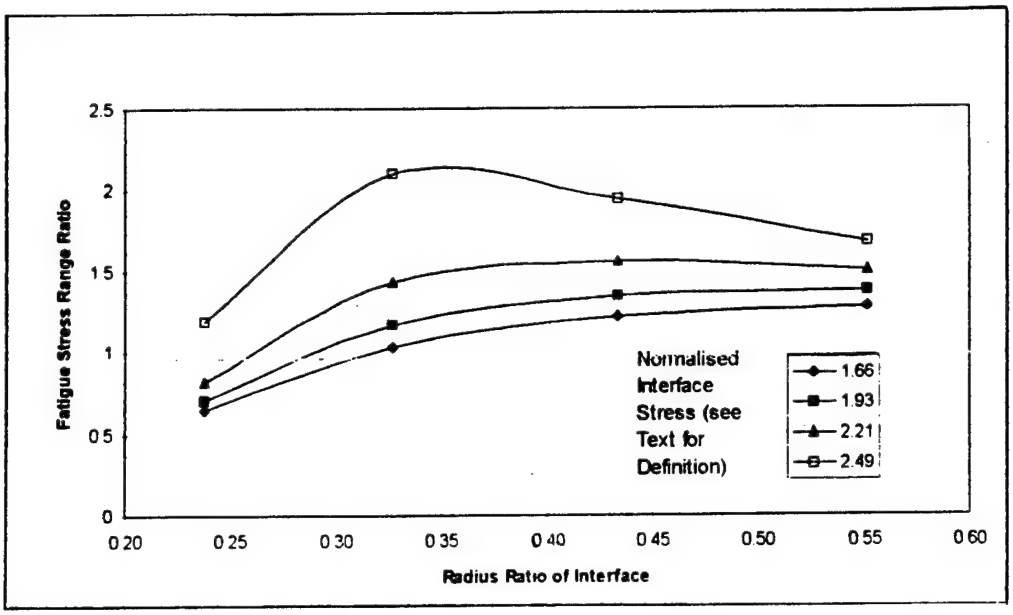

Figure 4 : Normalized Representation of Fatigue Stress Range Variation

As discussed earlier, the regions within which the R_σ surface shown in Fig. 4 dips below unity indicate a potential shift of failure location from bore to hole for the case of equal length initial defects at the two locations. In other cases the shift will occur in accordance with Equation (4).

SUMMARY AND CONCLUSIONS

This work addressed the fatigue lifetimes of thick cylinders containing multiple, axial holes within the wall. The holes are semi-circular and were created by thermally shrink-fitting an outer (plain) tube onto an inner tube which contains a periodic array of semi-circular notches. Finite Element analyses indicate that the residual stresses so introduced are compressive in the two principal potential failure locations, namely the bore and the notch root.

Superposition of an elastic stress field due to bore pressurization permits the calculation of positive cyclic stress ranges from bore to hole. This in turn may be used (after taking account of pressure infiltrating bore cracks) to calculate Fatigue Stress Ranges at bore and hole. These indicate that, for most cases considered, the critical fatigue location is the bore and that there is no benefit in seeking to reduce the stress concentration at the notch root.

Further comparison of an alternative method of introducing advantageous residual stresses, namely autofrettage of two of the cases considered, indicates significant lifetime advantages for the shrink-fit design.

Finally, a normalized design presentation is proposed which permits a rapid assessment of the major design parameters, interference and shrink-fit radius.

ACKNOWLEDGMENTS

Three of the authors (SNE, APP, and TJB) acknowledge partial support for this work via the European Research Office of the US Army Research, Development and Standardization Group (UK).

REFERENCES

[1] Underwood, J. H., and Parker, A. P., "Fatigue Life Analysis and Tests for Thick-Walled Cylinders Including Effects of Overstrain and Axial Grooves", ASME Conference on Pressure Vessels & Piping , Hawaii ,1995 (In Press), Published in ASME J Pressure Vessel Tech, Vol 117, 222-226 (1995)

[2] Parker, A. P. and Underwood, J. H., "Stress Concentration, Stress Intensity and Fatigue Crack Growth Along Evacuators of Pressurized, Autofrettaged Tubes", ASME PVP Conference Proceedings, Hawaii, 1995 (In Press) (Accepted for publication in ASME J Pressure Vessel Tech, 1996)

[3] Endersby, S. N., Bond, T. J. and Parker A. P., "Stress Concentration, Stress Intensity and Fatigue Crack Growth Along Angled Evacuators of Pressurized, Autofrettaged Tubes", (In preparation for publication, 1996)

[4] Parker, A. P., Endersby, S. N., Bond, T. J. and Underwood, J. H., Lee, S. L. and Higgins, J., "Stress Concentration, Stress Intensity and Fatigue Lifetime Calculations in Autofrettaged Tubes Containing Axial Perforations Within the Wall", ASME PVP Conference Proceedings, Montreal, July 1996 (In Press). (Submitted for publication in ASME J Pressure Vessel Tech, 1996)

[5] Parker, A P, Underwood, J H, "Some Methods of Representing Fatigue Lifetime as a Function of Stress Range and Initial Crack Length", presented at ASTM 28th National Symposium on Fatigue and Fracture Mechanics, Saratoga Springs, June 1996 (Submitted for publication in Fatigue and Fracture Mechanics: 28th Volume, ASTM STP 1321, J. H. Underwood and B. D. MacDonald, M. R. Mitchell, Eds., American Society for Testing and Materials, 1997)

TECHNICAL REPORT INTERNAL DISTRIBUTION LIST

	NO. OF COPIES
CHIEF, DEVELOPMENT ENGINEERING DIVISION	
ATTN: AMSTA-AR-CCB-DA	1
-DB	1
-DC	1
-DD	1
-DE	1
CHIEF, ENGINEERING DIVISION	
ATTN: AMSTA-AR-CCB-E	1
-EA	1
-EB	1
-EC	1
CHIEF, TECHNOLOGY DIVISION	
ATTN: AMSTA-AR-CCB-T	2
-TA	1
-TB	1
-TC	1
TECHNICAL LIBRARY	
ATTN: AMSTA-AR-CCB-O	5
TECHNICAL PUBLICATIONS & EDITING SECTION	
ATTN: AMSTA-AR-CCB-O	3
OPERATIONS DIRECTORATE	
ATTN: SIOWV-ODP-P	1
DIRECTOR, PROCUREMENT & CONTRACTING DIRECTORATE	
ATTN: SIOWV-PP	1
DIRECTOR, PRODUCT ASSURANCE & TEST DIRECTORATE	
ATTN: SIOWV-QA	1

NOTE: PLEASE NOTIFY DIRECTOR, BENÉT LABORATORIES, ATTN: AMSTA-AR-CCB-O OF ADDRESS CHANGES.

TECHNICAL REPORT EXTERNAL DISTRIBUTION LIST

	NO. OF COPIES
ASST SEC OF THE ARMY RESEARCH AND DEVELOPMENT ATTN: DEPT FOR SCI AND TECH THE PENTAGON WASHINGTON, D.C. 20310-0103	1
DEFENSE TECHNICAL INFO CENTER ATTN: DTIC-OCP (ACQUISITIONS) 8725 JOHN J. KINGMAN ROAD STE 0944 FT. BELVOIR, VA 22060-6218	2
COMMANDER U.S. ARMY ARDEC ATTN: AMSTA-AR-AEE, BLDG. 3022	1
AMSTA-AR-AES, BLDG. 321	1
AMSTA-AR-AET-O, BLDG. 183	1
AMSTA-AR-FSA, BLDG. 354	1
AMSTA-AR-FSM-E	1
AMSTA-AR-FSS-D, BLDG. 94	1
AMSTA-AR-IMC, BLDG. 59 PICATINNY ARSENAL, NJ 07806-5000	2
DIRECTOR U.S. ARMY RESEARCH LABORATORY ATTN: AMSRL-DD-T, BLDG. 305 ABERDEEN PROVING GROUND, MD 21005-5066	1
DIRECTOR U.S. ARMY RESEARCH LABORATORY ATTN: AMSRL-WT-PD (DR. B. BURNS) ABERDEEN PROVING GROUND, MD 21005-5066	1
DIRECTOR U.S. MATERIEL SYSTEMS ANALYSIS ACTV ATTN: AMXSY-MP ABERDEEN PROVING GROUND, MD 21005-5071	1
COMMANDER ROCK ISLAND ARSENAL ATTN: SMCRI-SEM ROCK ISLAND, IL 61299-5001	1
MIAC/CINDAS PURDUE UNIVERSITY 2595 YEAGER ROAD WEST LAFAYETTE, IN 47906-1398	1
COMMANDER U.S. ARMY TANK-AUTMV R&D COMMAND ATTN: AMSTA-DDL (TECH LIBRARY) WARREN, MI 48397-5000	1
COMMANDER U.S. MILITARY ACADEMY ATTN: DEPARTMENT OF MECHANICS WEST POINT, NY 10966-1792	1
U.S. ARMY MISSILE COMMAND REDSTONE SCIENTIFIC INFO CENTER ATTN: AMSMI-RD-CS-R/DOCUMENTS BLDG. 4484 REDSTONE ARSENAL, AL 35898-5241	2
COMMANDER U.S. ARMY FOREIGN SCI & TECH CENTER ATTN: DRXST-SD 220 7TH STREET, N.E. CHARLOTTESVILLE, VA 22901	1
COMMANDER U.S. ARMY LABCOM, ISA ATTN: SLCIS-IM-TL 2800 POWER MILL ROAD ADELPHI, MD 20783-1145	1

NOTE: PLEASE NOTIFY COMMANDER, ARMAMENT RESEARCH, DEVELOPMENT, AND ENGINEERING CENTER, BENÉT LABORATORIES, CCAC, U.S. ARMY TANK-AUTOMOTIVE AND ARMAMENTS COMMAND, AMSTA-AR-CCB-O, WATERVLIET, NY 12189-4050 OF ADDRESS CHANGES.

TECHNICAL REPORT EXTERNAL DISTRIBUTION LIST (CONT'D)

	NO. OF COPIES
COMMANDER U.S. ARMY RESEARCH OFFICE ATTN: CHIEF, IPO P.O. BOX 12211 RESEARCH TRIANGLE PARK, NC 27709-2211	1
DIRECTOR U.S. NAVAL RESEARCH LABORATORY ATTN: MATERIALS SCI & TECH DIV WASHINGTON, D.C. 20375	1
WRIGHT LABORATORY ARMAMENT DIRECTORATE ATTN: WL/MNM EGLIN AFB, FL 32542-6810	1
WRIGHT LABORATORY ARMAMENT DIRECTORATE ATTN: WL/MNMF EGLIN AFB, FL 32542-6810	1

NOTE: PLEASE NOTIFY COMMANDER, ARMAMENT RESEARCH, DEVELOPMENT, AND ENGINEERING CENTER, BENÉT LABORATORIES, CCAC, U.S. ARMY TANK-AUTOMOTIVE AND ARMAMENTS COMMAND, AMSTA-AR-CCB-O, WATERVLIET, NY 12189-4050 OF ADDRESS CHANGES.